Kinetic Study of OH + OH and OD + OD Reactions

Y. Bedjanian,* G. Le Bras, and G. Poulet

Laboratoire de Combustion et Systèmes Réactifs, CNRS and Université d'Orléans, 45071 Orléans Cedex 2, France

Received: April 6, 1999; In Final Form: June 14, 1999

The kinetics of the disproportionation reactions of OH and OD radicals, OH + OH → O + H_2O (1), OD + OD → O + D_2O (3), have been studied by the mass spectrometric discharge-flow method at temperatures between 233 and 360 K and at total pressure of 1 Torr of helium. The following Arrhenius expressions were obtained: $k_1 = (7.1 \pm 1.0) \times 10^{-13}\exp[(210 \pm 40)/T]$ and $k_3 = (2.5 \pm 0.5) \times 10^{-13}\exp[(170 \pm 60)/T]$ cm^3 molecule^{-1} s^{-1}. Reaction 4 between OH and OD radicals was also investigated and the same rate constant as for reaction 1 was measured. Both the observed temperature dependence of k_1 and the measured kinetic isotopic effect (k_1/k_3) are compatible with the mechanism proposed in a previous theoretical study (Harding, L. B.; Wagner, A. F. 22nd International Symposium on Combustion, 1988). In addition, a temperature-independent rate coefficient of $(1.20 \pm 0.25) \times 10^{-10}$ cm^3 molecule^{-1} s^{-1} was measured for the reaction D + NO_2 → OD + NO in the temperature range 230−365 K.

Introduction

OH radicals are important intermediate species in gas-phase combustion and atmospheric processes. It is not surprising that the kinetics of OH reactions have been studied very extensively in the past. For example, there are about 800 reactions of OH compiled in the NIST data base.[1] The disproportionation reaction of OH radicals has been also studied in many laboratories:[2−18]

$$OH + OH \rightarrow O + H_2O \quad (1)$$

$$OH + OH (+M) \rightarrow H_2O_2 (+M) \quad (1')$$

The kinetics of these reactions have been investigated at high temperature ($T = 1050-2380$ K)[2−4] and at room temperature,[5−13] and a temperature dependence study[14] has been carried out at $T = 250-580$ K. The pressure dependence of the rate constant of the reaction, which possesses one pressure-dependent channel (reaction 1′), has been also investigated.[12,15−18] Besides, the temperature dependence of the rate constant of reaction 1 calculated in an ab initio study[19] is in good agreement with all experimental data between 300 and 2000 K. However, some uncertainties still remain. First, the value of k_1 even at room temperature lies between 1.4×10^{-12} and 2.3×10^{-12} cm^3 molecule^{-1} s^{-1} (e.g., ref 20). Second, the temperature dependence of the rate constant in the low-temperature range has been measured in only one study.[14] Such uncertainties are revealed by recent compilations of kinetic data for atmospheric chemistry,[20,21] which propose different recommendations for the temperature dependence of k_1: $E/R = (240 \pm 240)$ K,[20] based on the results of ref 14 and a negative temperature dependence of k_1 (at low temperatures)[21] based on the theoretical calculations.[19]

Accurate kinetic information on reaction 1 at high temperatures is important for modeling of combustion processes, where high OH concentrations may make this reaction significant. Although the OH + OH reaction is negligible in atmospheric processes (because of the low OH concentrations), low-temperature data are important for laboratory studies of OH reactions of atmospheric relevance. For example, the present study has been triggered by that of the reaction of OH with BrO radicals:

$$OH + BrO \rightarrow HO_2 + Br \quad (2a)$$

$$\rightarrow HBr + O_2 \quad (2b)$$

The potential occurrence of channel 2b is of great importance for the stratospheric bromine partitioning.[22,23] Hence, the experimental determination of the branching ratio for channel 2b is required. From the unique study of reaction 2,[24] and considering that the branching ratio of channel 2b is likely to be as low as a few percentages, it appears that one cannot neglect the side and secondary processes involved in the reactive system used to produce OH and BrO radicals. Thus, accurate kinetic data for all these reactions are needed. In a preliminary study,[25] the kinetic parameters for the reactions of OH and OD with Br_2 have been measured. In the present paper, the temperature dependence of the OH disproportionation reaction has been measured at low pressure:

$$OH + OH \rightarrow O + H_2O \qquad \Delta H = -16.8 \text{ kcal mol}^{-1} \quad (1)$$

Unless specified, the heats of formation of species used are from ref 20.

The isotopic substitution is known to be adapted in kinetic studies, especially for the determination of reaction products. Isotopic labeling experiments have been performed in a recent study of the OH and OD + ClO reactions[26] for the determination of the branching ratio of the minor HCl- or DCl-forming channel. In relation with these OD reactions, reaction 3 has been also investigated:

$$OD + OD \rightarrow O + D_2O \qquad \Delta H = -17.5 \text{ kcal mol}^{-1} \quad (3)$$

(The heats of formation for deuterium-containing species are from ref 27.)

10.1021/jp991146r CCC: $18.00
Published on Web 08/18/1999

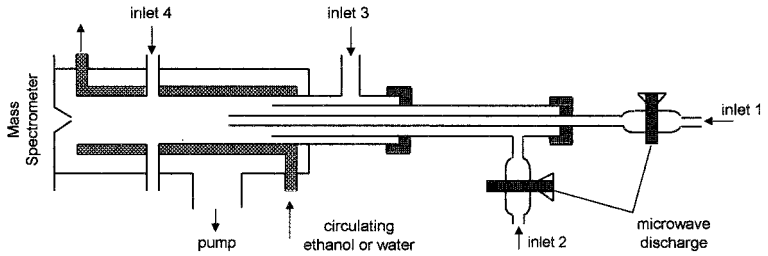

Figure 1. Diagram of the apparatus used.

Only one kinetic determination at room temperature is available for this reaction.[28] In fact, the kinetic database for reactions of isotopically substituted species is rather scarce. Finally, to provide a complete data set the cross-reaction between OH and OD radicals has been also studied:

$$OH + OD \rightarrow O + HDO \qquad \Delta H = -17.1 \text{ kcal mol}^{-1} \quad (4)$$

In addition, kinetic data for the reaction of D atoms with NO_2, used as a source of OD radicals, have been obtained for the first time:

$$D + NO_2 \rightarrow OD + NO \qquad \Delta H = -30.6 \text{ kcal mol}^{-1} \quad (5)$$

Experimental Section

Experiments were carried out in a discharge flow reactor using a modulated molecular beam mass spectrometer as a detection method. The main reactor, shown in Figure 1 along with the movable injector for the reactants, consisted of a Pyrex tube (45 cm length and 2.4 cm i.d.) with a jacket for the thermostated liquid circulation (water or ethanol). The walls of the reactor as well as of the injector were coated with halocarbon wax to minimize the heterogeneous loss of active species. All experiments were conducted at 1 Torr total pressure, with helium being used as the carrier gas.

The fast reaction of hydrogen atoms with NO_2 was used as a source of OH radicals, H atoms being produced in a microwave discharge of H_2/He mixture:

$$H + NO_2 \rightarrow OH + NO \quad (6)$$

$$k_6 = 4.0 \times 10^{-11}\exp(-340/T)\text{cm}^3 \text{ molecule}^{-1} \text{ s}^{-1} \quad \text{(ref 20)}$$

Similarly, the reaction of D atoms with NO_2 was used to produce OD radicals:

$$D + NO_2 \rightarrow OD + NO \quad (5)$$

$$k_5 = (1.20 \pm 0.25) \times 10^{-11} \text{ cm}^3 \text{ molecule}^{-1} \text{ s}^{-1} \quad (T = 230-365 \text{ K}) \text{ (this study)}$$

NO_2 was always used in excess over H and D atoms. OH and OD radicals were detected as $HOBr^+$(m/e = 96/98) and $DOBr^+$(m/e = 97/99) respectively, after scavenging by an excess of Br_2 (added at the end of the reactor through inlet 4, located 5 cm upstream of the sampling cone) via reactions 7 and 8, respectively:

$$OH + Br_2 \rightarrow Br + HOBr \quad (7)$$

$$k_7 = (1.8 \pm 0.3) \times 10^{-11}\exp[(235 \pm 50)/T] \text{ cm}^3 \text{ molecule}^{-1} \text{ s}^{-1} \text{ (ref 25)}$$

$$k_7 = (1.97 \pm 0.32) \times 10^{-11}\exp[(240 \pm 62)/T] \text{ cm}^3 \text{ molecule}^{-1} \text{ s}^{-1} \text{ (ref 29)}$$

$$OD + Br_2 \rightarrow Br + DOBr \quad (8)$$

$$k_8 = (1.9 \pm 0.2) \times 10^{-11}\exp[(220 \pm 25)/T] \text{ cm}^3 \text{ molecule}^{-1} \text{ s}^{-1} \text{ (ref 25)}$$

This method of OH and OD detection was preferred to the direct detection of these radicals at m/e = 17 (OH^+) and m/e = 18 (OD^+) because of significant contributions of traces of water vapor. The same procedure of OH(OD) chemical conversion to HOBr(DOBr) was used for the measurements of the absolute radical concentrations: [OH] = [HOBr] = $\Delta[Br_2]$ (or [OD] = [DOBr] = $\Delta[Br_2]$). Thus, OH(OD) concentrations were determined from the consumed fraction of $[Br_2]$. $[Br_2]$ was determined from the flow rate of known Br_2/He mixtures. The method used for this HOBr(DOBr) detection and their absolute calibrations requires that secondary reactions be negligible. For example, in the case of OH radicals, possible secondary reactions following reaction 7 are:

$$OH + HOBr \rightarrow \text{products} \quad (9)$$

$$OH + Br \rightarrow O + HBr \quad \Delta H = 14.9 \text{ kcal mol}^{-1} \quad (10a)$$

$$\rightarrow H + BrO \quad \Delta H = 44.7 \text{ kcal mol}^{-1} \quad (10b)$$

$$\rightarrow HOBr\ (+M) \quad \Delta H = -50 \text{ kcal mol}^{-1} \quad (10c)$$

$$Br + HOBr \rightarrow OH + Br_2 \quad (11a)$$

$$\Delta H = (4.0 \pm 2.0) \text{ kcal mol}^{-1}$$

$$\rightarrow BrO + HBr \quad (11b)$$

$$\Delta H = (4.2 \pm 3.4) \text{ kcal mol}^{-1}$$

(The heat of formation of BrO radicals, $\Delta H_f(BrO) = (28.6 \pm 1.4)$ kcal mol^{-1}, is from ref 30.) It has been shown that reaction 9 is slow, the upper limit for the rate constant being: $k_9 \leq 5 \times 10^{-13}$ cm^3 molecule^{-1} s^{-1} (at T = 300 K).[31] Considering this value and the fact that OH is rapidly consumed in reaction 1 (at the high Br_2 concentrations used), reaction 9 was negligible in the present experiments. The bimolecular channels of reaction 10 are too endothermic to proceed with a significant rate, and the association channel (10c) could also be considered as negligible at the low pressure (1 Torr) used. Finally, both channels of reaction 11 are endothermic and are likely of minor importance. The same conclusions apply for the case of OD radicals. Because relatively high concentrations of OH and OD were used in the calibration experiments, the O atoms produced in reactions 1 and 3 could react with Br_2, and the possible

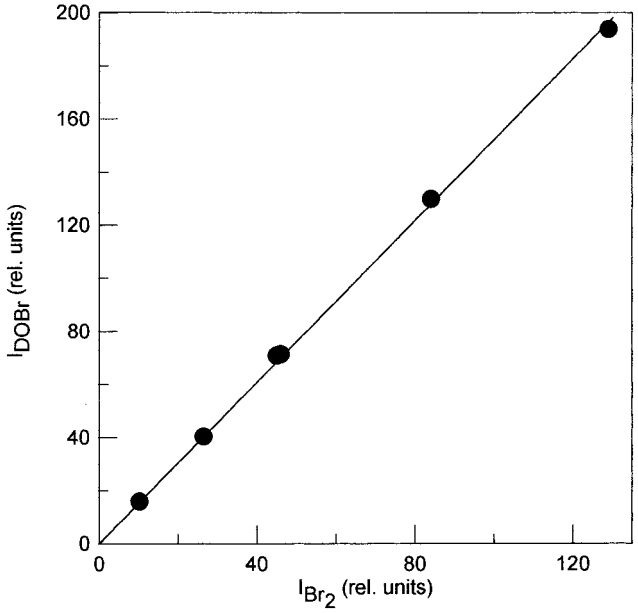

Figure 2. Example of calibration curve for DOBr (see text): DOBr formed in the OD + Br_2 reaction as a function of Br_2 consumed (in relative units).

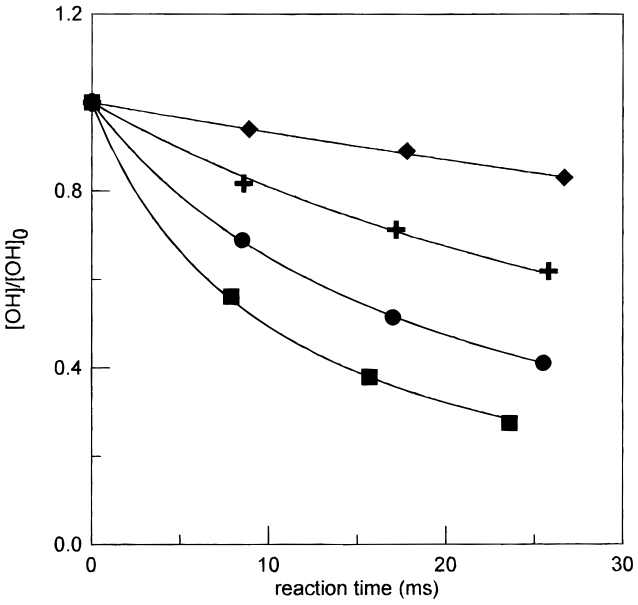

Figure 3. Reaction OH + OH → O + H_2O (1): example of experimental (points) and simulated (solid lines) decays of OH for different initial concentrations (T = 299 K): $[OH]_0$ = 34.3 (■), 16.1 (●), 6.4 (+), and 0.34 (◆) × 10^{12} molecules cm^{-3}.

contribution of this O + Br_2 reaction should be considered:

$$O + Br_2 \rightarrow BrO + Br \quad (12)$$

$$k_{12} = 1.76 \times 10^{-11}\exp(40/T)\ cm^3\ molecule^{-1}\ s^{-1} \quad (ref\ 32)$$

In fact, O atoms, formed in reaction 1 (in the case of OH + Br_2 reaction) and consumed mainly in reactions with OH (13) and NO_2 (14), reach steady-state concentration: $[O]_{ss} = k_1[OH]^2/(k_{13}[OH] + k_{14}[NO_2])$:

$$O + OH \rightarrow H + O_2 \quad (13)$$

$$k_{13} = 2.2 \times 10^{-11}\exp(120/T)\ cm^3\ molecule^{-1}\ s^{-1} \quad (ref\ 20)$$

$$O + NO_2 \rightarrow NO + O_2 \quad (14)$$

$$k_{14} = 6.5 \times 10^{-12}\exp(120/T)\ cm^3\ molecule^{-1}\ s^{-1} \quad (ref\ 20)$$

Under the typical conditions of the calibration experiments ($[OH]_{max} \cong 10^{13}$ molecules cm^{-3} and $[NO_2] \cong 5 \times 10^{13}$ molecules cm^{-3}), the steady-state concentration of O atoms was lower than 0.02 × [OH]. Therefore the contribution of O + Br_2 reaction in the consumption of Br_2 was negligible. The same conclusion can be driven for the OD calibration, because the O-forming reaction OD + OD has a rate constant around three times lower than that of the OH + OH reaction (this study). An example of calibration plot for [DOBr] is shown in Figure 2. The linear dependence observed for the signal of DOBr on the fraction of Br_2 consumed in reaction 3 ($\Delta[Br_2]$ being changed by more than one order of magnitude) demonstrates the negligible role of secondary chemistry.

The same procedure as above was used for the detection and measurements of the absolute concentrations of H and D atoms. Br_2 was added at the end of the reactor (inlet 4) to convert H and D atoms into HBr and DBr, respectively via reactions 15 and 16:

$$H + Br_2 \rightarrow Br + HBr \quad (15)$$

$$k_{15} = 6.7 \times 10^{-10}\exp(-673/T)\ cm^3\ molecule^{-1}\ s^{-1} \quad (ref\ 33)$$

$$D + Br_2 \rightarrow Br + DBr \quad (16)$$

$$k_{16} = 6.0 \times 10^{-10}\exp(-709/T)\ cm^3\ molecule^{-1}\ s^{-1} \quad (ref\ 33)$$

Absolute concentrations of H and D atoms were determined as: [H] = [HBr] = $\Delta[Br_2]$ or [D] = [DBr] = $\Delta[Br_2]$.

The purities of the gases used were as follows: He > 99.9995% (Alphagaz), was passed through liquid nitrogen traps; H_2 > 99.998% (Alphagaz); D_2 > 99.7% (Alphagaz); Br_2 > 99.99% (Aldrich); NO_2 > 99% (Alphagaz).

Results

Reaction OH + OH → O + H_2O. Reaction 1 was studied in the temperature range 233−360 K. OH radicals were produced directly in the main reactor through reaction 6, H atoms and NO_2 being introduced through the movable inlet 1 and the fixed inlet 3, respectively. High initial concentrations of NO_2 were used {$[NO_2]_0 = (3-20) \times 10^{13}$ molecules cm^{-3}}, leading to a fast disappearance of H atoms, as verified by the detection of HBr (Br_2 being added at the end of the reactor: see previous section). OH decay kinetics were measured for different initial concentrations of the radicals. To derive the rate constant k_1, these kinetic runs were simulated using a simplified two-step mechanism:

$$OH + OH \rightarrow O + H_2O \quad (1)$$

$$OH \rightarrow loss \quad (17)$$

The possible secondary reaction 13 between O atoms and OH radicals did not contribute to the OH consumption, because the H atoms formed in this reaction were rapidly converted back to OH by the NO_2 used in excess: $[NO_2] = (2.5-5) \times 10^{13}$ molecules cm^{-3}. The rate of reaction 17 was measured directly in independent experiments using low initial concentrations of OH: $[OH] = (2-4) \times 10^{11}$ molecules cm^{-3}. After a small

TABLE 1: Experimental Conditions and Results of the Reaction OH + OH → O + H_2O (1)

$T = 360$ K		$T = 340$ K		$T = 320$ K		$T = 299$ K		$T = 273$ K		$T = 253$ K		$T = 233$ K	
$[OH]_0$[a]	k_1[b]	$[OH]_0$	k_1	$[OH]_0$	k_1	$[OH]_0$	k_1	$[OH]_0$	k_1	$[OH]_0$	k_1	$[OH]_0$	k_1
9.1	1.29	7.0	1.31	4.5	1.37	3.5	1.42	2.2	1.54	4.4	1.54	2.9	1.77
11.7	1.26	9.4	1.33	8.2	1.27	6.4	1.30	5.0	1.54	6.7	1.47	5.2	1.53
18.5	1.26	11.8	1.26	11.2	1.31	11.3	1.45	8.8	1.63	9.8	1.58	8.2	1.78
30.8	1.39	17.9	1.31	12.1	1.30	14.7	1.41	13.2	1.54	13.0	1.62	9.5	1.60
40.5	1.22	24.8	1.31	15.1	1.37	16.1	1.44	16.3	1.59	16.6	1.54	12.1	1.74
49.3	1.29	34.0	1.31	18.2	1.40	23.1	1.44	20.6	1.58	19.5	1.54	14.8	1.67
66.4	1.26	40.6	1.27	24.2	1.37	25.3	1.37	23.6	1.67	25.0	1.63	17.8	1.88
		50.3	1.25	30.6	1.35	28.9	1.38	29.8	1.60	31.6	1.59	20.7	1.75
				37.5	1.33	34.3	1.36					24.6	1.84
												33.7	1.77
												37.4	1.76
k_1[c] = 1.28 ± 0.18		$k_1 = 1.29 \pm 0.16$		$k_1 = 1.34 \pm 0.17$		$k_1 = 1.40 \pm 0.19$		$k_1 = 1.59 \pm 0.21$		$k_1 = 1.56 \pm 0.21$		$k_1 = 1.74 \pm 0.27$	

[a] Concentrations are in 10^{12} molecule cm^{-3} units. [b] Rate constants are in 10^{-12} cm^3 $molecule^{-1}$ s^{-1} units. [c] Mean values of the rate constants in 10^{-12} cm^3 $molecule^{-1}$ s^{-1} units; the error is the statistical uncertainty with addition of 10% for systematic errors.

correction due to the contribution of reaction 1, the measured values of k_{17} were in the range 4−16 s^{-1} and increased with increasing $[NO_2]$ and decreasing temperature. Typical examples of experimental and simulated decays of OH are shown in Figure 3. All the conditions and results for the measurements of k_1 are summarized in Table 1. The temperature dependence of k_1 is shown in Figure 4. The Arrhenius expression for k_1 derived from a least-squares fit to the experimental data is:

$$k_1 = (7.1 \pm 1.0) \times 10^{-13}\exp[(210 \pm 40)/T]\ \text{cm}^3\ \text{molecule}^{-1}\ \text{s}^{-1}$$

Quoted uncertainties represent two standard deviations.

In the determination of k_1, the rate of reaction 17 measured at low initial concentrations of OH was considered as constant for the entire range of $[OH]_0$ used. In fact, reaction 17 is a combination of several processes: the heterogeneous OH loss, the reaction of OH with NO_2 (18), and the possible secondary reaction between OH and HNO_3 (19):

$$\text{OH} + \text{NO}_2\ (+\text{M}) \rightarrow \text{HNO}_3\ (+\text{M}) \qquad (18)$$

$$k_{18} = 2.5 \times 10^{-30}(T/300)^{-4.4}\ \text{cm}^6\ \text{molecule}^{-2}\ \text{s}^{-1}\ (\text{for M} = \text{N}_2)\ (\text{ref 20})$$

$$\text{OH} + \text{HNO}_3\ (+\text{M}) \rightarrow \text{H}_2\text{O} + \text{NO}_3\ (+\text{M}) \qquad (19)$$

$$k_{19} = 7.2 \times 10^{-15}\exp(785/T)\ \text{cm}^3\ \text{molecule}^{-1}\ \text{s}^{-1}\ (\text{ref 20})$$

k_{19} is pressure dependent, and the expression given here is the low-pressure (bimolecular) limit of the rate constant.[20] In the present study, k_{19} lies between 6.4×10^{-14} ($T = 360$ K) and 2.1×10^{-13} cm^3 $molecule^{-1}$ s^{-1} ($T = 233$ K). To estimate the contribution of reaction 19 in the OH loss rate, numerical simulations have been performed. It was observed that, even at the lowest temperature of this study ($T = 233$ K), that is, for the maximum values of the rate constants of reactions 18 and 19, the contribution of reaction 19 to OH loss rate was negligible (<5%) compared to the OH loss due to the heterogeneous reaction and to reaction 18. In these calculations, the value of k_{18} given above was used. The value of k_{18} with He as a third body can be lower by a factor 2 to 3[1]. For example, the rate constant of the similar reaction of OD radicals with NO_2 is: 4.05×10^{-30} and 1.27×10^{-30} cm^6 $molecule^{-2}$ s^{-1} for M = N_2 and He, respectively.[34] Hence, the influence of reaction 19 could be disregarded and the rate constant of reaction 17 can be written as: $k_{17} = k_{wall} + k_{18}[NO_2]_{mean}$, independent of the initial OH concentration. The concentration of NO_2 along the reaction zone ($[NO_2]_{mean}$) was kept quasi-constant for all the kinetic runs of OH, at a given temperature, with a mean value taking into account the consumption of NO_2 due to reactions 18 and 14 and to the reaction sequence 13 + 6. Finally, as one can see from Table 1, the values obtained for k_1 were not sensitive within experimental uncertainty to the initial concentration of OH, which shows that the OH loss processes were analyzed correctly.

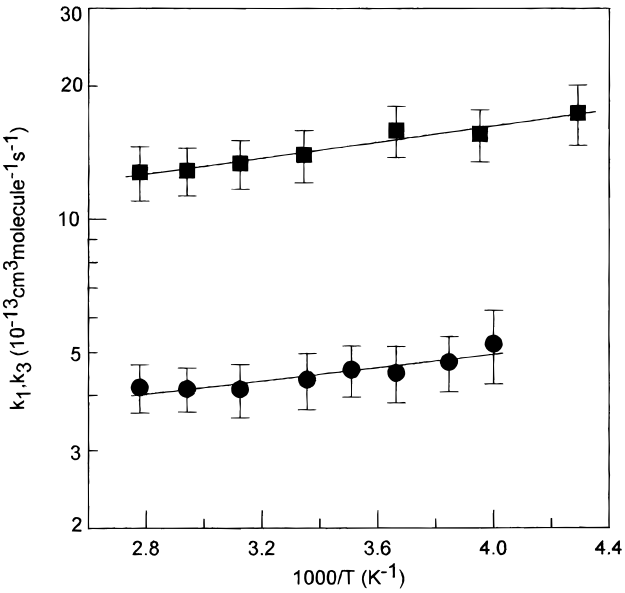

Figure 4. Temperature dependence of the rate constants for reactions 1 and 3: OH + OH → O + H_2O (■) and OD + OD → O + D_2O (●).

Reaction OD + OD → O + D_2O. This disproportionation reaction was studied in the same way as described above for the OH + OH reaction. OD radicals were produced via reaction 5 and were detected at $m/e = 97/99$ (as $DOBr^+$). As in the case of OH, the experimental OD decays were simulated, using a two-step mechanism:

$$\text{OD} + \text{OD} \rightarrow \text{O} + \text{D}_2\text{O} \qquad (3)$$

$$\text{OD} \rightarrow \text{loss} \qquad (20)$$

Reaction 2 was also taken as the combination of two processes leading to OD consumption, the OD heterogeneous loss and its reaction with NO_2:

$$\text{OD} + \text{NO}_2\ (+\text{M}) \rightarrow \text{DNO}_3\ (+\text{M}) \qquad (21)$$

$$k_{21} = 1.27 \times 10^{-30}\ \text{cm}^6\ \text{molecule}^{-2}\ \text{s}^{-1}$$
$$(T = 300\ \text{K, M} = \text{He})^{34}$$

Similarly to OH reactions 13 and 19, secondary OD reactions 22 and 23 were negligible:

$$\text{OD} + \text{DNO}_3\ (+\text{M}) \rightarrow \text{D}_2\text{O} + \text{NO}_3\ (+\text{M}) \qquad (22)$$

$$k_{22} = 5.27 \times 10^{-15}\exp(241/T)\ \text{cm}^3\ \text{molecule}^{-1}\ \text{s}^{-1}$$
(ref 35)

$$\text{O} + \text{OD} \rightarrow \text{D} + \text{O}_2 \qquad (23)$$

The values of k_{20} measured at low concentrations of OD and used in the calculations were in the range $3-15\ \text{s}^{-1}$, depending on the NO_2 concentration and on the temperature. All the results obtained for k_3 for the various ranges of initial OD concentrations are summarized in Table 2. The Arrhenius expression of k_3, corresponding to the experimental data shown in Figure 4, is:

$$k_3 = (2.5 \pm 0.5) \times 10^{-13}\exp[(170 \pm 60)/T]\ \text{cm}^3\ \text{molecule}^{-1}\ \text{s}^{-1}$$

Quoted uncertainties represent two standard deviations.

Reaction OH + OD → O + HOD. The cross-reaction between OH and OD was studied at three temperatures: 273, 298, and 320 K. OH and OD radicals were formed simultaneously in the main reactor via reactions 6 and 5, respectively. H and D atoms were produced in a microwave discharge of H_2/D_2/He mixtures and introduced into the reactor through inlet 1, with NO_2 flow through inlet 3. As in previous experiments, Br_2 (at concentrations around 1×10^{14} molecules cm^{-3}) was added at the end of the reactor (inlet 4), and OH and OD were detected as HOBr and DOBr, respectively. Experiments were carried out in excess of OD radicals over OH. The concentrations used for the reactants were: $[NO_2]_{\text{mean}} \cong 5 \times 10^{13}$, $[OH]_0 = (4-6) \times 10^{11}$, and $[OD]_0 = (2.5-7.9) \times 10^{12}$ molecules cm^{-3}. The linear flow velocity was in the range $780-1000\ \text{cm s}^{-1}$. The consumption of both reactants (OH and OD) was measured. The disproportionation reaction 3, the heterogeneous loss, and the reaction with NO_2 were the main processes responsible for the observed decays of OD. The consumption of OH was mainly due to the OH + OD reaction, the OH wall loss, and the reaction with NO_2. The contribution of the OH + OH reaction could be considered as negligible because of relatively low $[OH]_0$ used. To derive the value of k_4, the experimental OH decays were simulated using the experimental profiles of [OD] and the simple kinetic mechanism:

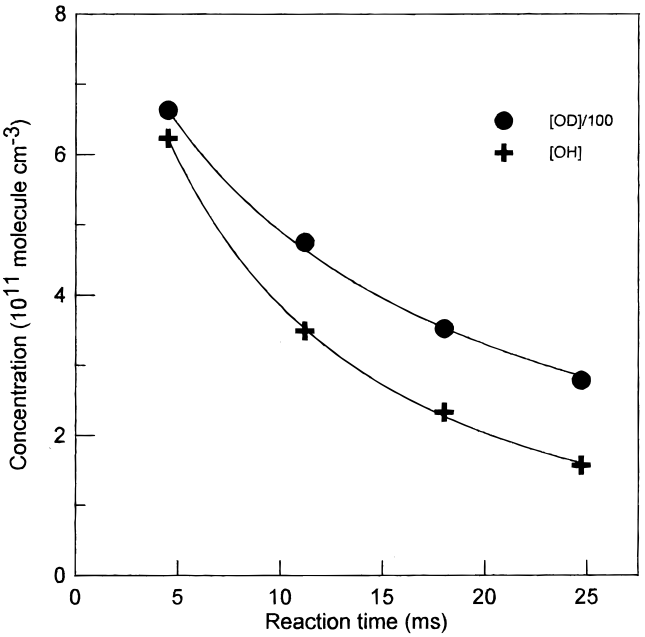

Figure 5. Reaction OH + OD → O + HDO (4): example of experimental (points) and simulated (solid lines) kinetics of OH and OD radicals.

$$\text{OH} + \text{OD} \rightarrow \text{O} + \text{HDO} \qquad (4)$$

$$\text{OH} \rightarrow \text{loss} \qquad (17)$$

As already discussed in the previous sections, the rate of the process 17 was measured separately in the absence of OD radicals and ranged between 8 and $10\ \text{s}^{-1}$. An example of experimental and simulated kinetics of OH and OD is shown in Figure 5. All the results obtained for k_4 are given in Table 3. The values thus measured for k_4 are the same (within uncertainty limits) as those measured above for the OH + OH reaction.

Reaction D + NO_2 → OD + NO. In this series of experiments, D atoms were formed in the discharge of D_2/He mixtures and introduced into the reactor through the movable injector (inlet 1), NO_2 flowed through inlet 3, and Br_2 was added at the end of the reactor (inlet 4). The detection of H, D, OH,

TABLE 2: Experimental Conditions and Results of the Reaction OD + OD → O + D_2O (3)

$T = 360$ K		$T = 340$ K		$T = 320$ K		$T = 298$ K		$T = 285$ K		$T = 273$ K		$T = 260$ K		$T = 250$ K	
$[OD]_0$[a]	k_3[b]	$[OD]_0$	k_3	$[OD]_0$	k_3	$[OD]_0$	k_3	$[OD]_0$	k_3	$[OD]_0$	k_3	$[OD]_0$	k_3	$[OD]_0$	k_3
13.9	4.20	12.6	4.19	5.9	4.00	14.4	4.16	12.1	4.66	13.2	4.78	5.6	4.72	10.2	5.66
19.2	4.30	12.6	4.13	9.2	3.84	23.6	4.23	25.0	4.77	18.0	4.48	14.9	4.47	10.4	4.67
25.7	4.02	22.4	4.17	14.3	4.29	35.7	4.39	36.0	4.46	27.5	4.52	20.5	4.58	15.7	5.00
40.4	4.29	33.1	4.02	21.3	4.01	41.4	4.13	40.6	4.43	33.5	4.47	34.1	4.71	17.8	4.73
56.2	4.11	51.6	4.10	25.9	4.27	53.8	4.49	68.9	4.76	40.8	4.20	40.4	4.95	20.8	5.61
71.3	4.08	62.8	4.15	32.1	4.27	63.5	4.58	74.5	4.46	48.6	4.31	51.0	5.0	21.6	5.55
85.1	4.19	88.4	4.16	43.1	4.10	67.2	4.58	84.7	4.46	54.0	4.76	64.9	4.44	29.2	5.70
105.0	4.20	102.1	4.17	52.8	4.19	77.7	4.42					72.4	4.81	35.8	4.48
				63.3	4.19	83.0	4.09					81.3	4.86	39.6	4.73
												91.7	5.0	46.7	5.13
														47.8	5.39
														55.2	5.56
														57.3	5.00
														65.0	5.99
k_3[c] = 4.17 ± 0.52		$k_3 = 4.14 \pm 0.47$		$k_3 = 4.13 \pm 0.57$		$k_3 = 4.34 \pm 0.63$		$k_3 = 4.57 \pm 0.61$		$k_3 = 4.50 \pm 0.66$		$k_3 = 4.75 \pm 0.68$		$k_3 = 5.23 \pm 0.99$	

[a] Concentrations are in 10^{12} molecules cm^{-3} units. [b] Rate constants are in $10^{-13}\ \text{cm}^3\ \text{molecule}^{-1}\ \text{s}^{-1}$ units. [c] Mean values of the rate constants in $10^{-13}\ \text{cm}^3\ \text{molecule}^{-1}\ \text{s}^{-1}$ units; the error is the statistical uncertainty with addition of 10% for systematic errors.

TABLE 3: Experimental Conditions and Results of the Reaction OH + OD → O + HOD (4)

$T = 320$ K		$T = 298$ K		$T = 273$ K	
$[OD]_0$[a]	k_4[b]	$[OD]_0$	k_4	$[OD]_0$	k_4
5.8	1.31	5.4	1.44	2.5	1.28
9.3	1.15	11.8	1.45	6.0	1.65
13.5	1.46	18.6	1.65	11.6	1.73
18.3	1.51	25.8	1.67	20.4	1.68
31.9	1.21	37.2	1.57	30.7	1.61
38.7	1.27	48.4	1.54	35.6	1.59
45.3	1.22	60.5	1.35	53.8	1.51
60.3	1.12	66.3	1.40	79.3	1.20
k_4[c] = 1.28 ± 0.27		$k_4 = 1.51 \pm 0.27$		$k_4 = 1.53 \pm 0.35$	

[a] Concentrations are in 10^{12} molecules cm^{-3} units. [b] Rate constants are in 10^{-12} cm^3 molecule^{-1} s^{-1} units. [c] Mean values of the rate constants in 10^{-12} cm^3 molecule^{-1} s^{-1} units; the error is the statistical uncertainty with addition of 10% for systematic errors.

TABLE 4: Experimental Conditions and Results of the Reaction D + NO_2 → OD + NO (5)

N[a]/exp	T (K)	$[D]_0$[b]	$[NO_2]_0$[b]	k_5[c]
5	365	0.2−0.4	0.6−6.5	1.09 ± 0.16 (d)
7	365	0.9−7.1	0.4−0.5	1.07 ± 0.14 (e)
5	360	0.3−0.5	0.7−7.1	1.24 ± 0.15 (d)
6	360	0.9−6.9	0.4−0.6	1.17 ± 0.14 (e)
5	320	0.2−0.4	0.4−7.8	1.30 ± 0.17 (d)
6	320	0.4−6.4	0.3−0.5	1.24 ± 0.16 (e)
5	296	0.2−0.4	0.3−7.0	1.28 ± 0.16 (d)
10	296	0.5−6.4	0.4−0.6	1.28 ± 0.16 (e)
7	273	0.4−7.0	0.3−0.7	1.28 ± 0.14 (e)
6	250	0.3−0.5	0.5−7.7	1.28 ± 0.17 (d)
8	250	0.5−6.6	0.4−0.8	1.11 ± 0.13 (e)
6	230	0.4−0.5	0.5−6.7	1.15 ± 0.16 (d)
6	230	0.4−6.4	0.4−0.7	1.21 ± 0.16 (e)

[a] Number of kinetic runs. [b] Concentrations are in 10^{12} molecules cm^{-3} units. [c] Rate constants are in 10^{-10} cm^3 molecule^{-1} s^{-1} units; the error is 1σ with addition of 10%; the letter in parentheses indicates the experimental conditions used (see text): D decay kinetics in excess of NO_2 (d) and NO_2 decay kinetics in excess of D atoms (e).

and OD was made at the mass of HBr^+, DBr^+, $HOBr^+$, and $DOBr^+$, respectively.

The rate constant of reaction 5 was measured from both the kinetics of D atom decays monitored in excess of NO_2 and the NO_2 kinetics with an excess of D atoms. The ranges of the reactant concentrations used in these experiments are shown in Table 4. The flow velocity in the reactor was 1600−2600 cm s^{-1}. Figure 6 shows pseudo-first-order plots obtained from NO_2 and D atom decay kinetics in excess of D and NO_2, respectively. The measured values of the pseudo-first-order rate constants, $k_5' = k_5[D]$ and $k_5' = k_5[NO_2]$ (the rate of the heterogeneous loss of D atoms was found to be negligible, < 3 s^{-1}), were corrected for axial and radial diffusion.[36] For the diffusion coefficient of D atom in He, the value of D_{H2-He} [37] was used. D_{NO2-He} was calculated from D_{CO2-He}.[37] The maximum correction for k_5' was 25%. All the results are given in Table 4. No dependence of k_5 with temperature was observed in the T range investigated, leading to the final value:

$$k_5 = (1.20 \pm 0.25) \times 10^{-10} \text{ cm}^3 \text{ molecule}^{-1} \text{ s}^{-1} \quad (T = 230-365 \text{ K})$$

Other series of experiments were carried out in which k_5 was measured by a relative method, using the reaction of H atoms with NO_2 as the reference. Two approaches were used. In the first one, the kinetics of H and D atoms decays in excess of NO_2 were observed simultaneously and the ratio of the rate constants k_6/k_5 was simply (the heterogeneous losses of H and D atoms were negligible):

$$\ln\frac{[H]_0}{[H]} = \frac{k_6}{k_5}\ln\frac{[D]_0}{[D]}$$

where $[H]_0$ and $[D]_0$ are the initial concentrations of H and D atoms. In the second series of runs, the kinetics of OH and OD formation in reactions 6 and 5, respectively, were measured and the ratio of the rate constants was derived from the same expression as above with $[H]_0 = [OH]_\infty$ ($[D]_0 = [OD]_\infty$), measured at high concentrations of NO_2 after complete titration of the atoms, and $[H] = [OH]_\infty - [OH]$ ($[D] = [OD]_\infty - [OD]$). The initial concentrations of the reactants were: $[H]_0$ and $[D]_0$ in the range $(2-5) \times 10^{11}$ and $[NO_2]_0 = (2-7) \times 10^{12}$ molecules cm^{-3}. Under these experimental conditions, the secondary reactions 24 and 25 were neglected:

$$\text{D} + \text{OH} \rightarrow \text{H} + \text{OD} \qquad (24)$$

$$k_{24} = 5.25 \times 10^{-11} (T/298)^{-0.63} \text{cm}^3 \text{ molecule}^{-1} \text{ s}^{-1} \quad \text{(ref 38)}$$

$$\text{H} + \text{OD} \rightarrow \text{D} + \text{OH} \qquad \Delta H = 1.45 \text{ kcal mol}^{-1} \quad (25)$$

The obtained results are given in Figure 7, which shows a good agreement between two series of kinetics, either from reactant consumption or from product formation. It is also observed that the k_6/k_5 ratio does not depend on temperature (for $T = 298$ and 230 K) within the experimental uncertainty. The final value of this ratio is:

$$k_6/k_5 = 1.06 \pm 0.05 \ (T = 230-298 \text{ K})$$

The error is twice the standard deviation. Combining this ratio with the recommended expression for k_6: $k_6 = 4.0 \times 10^{-11}$ exp[(−340 ± 300)/T] cm^3 molecule^{-1} s^{-1},[20] the values of k_5 are: $k_5 = 1.2 \times 10^{-11}$ and 0.9×10^{-11} cm^3 molecule^{-1} s^{-1} at $T = 296$ and 230 K, respectively. These values are consistent with those obtained in the absolute measurements, although a temperature dependence was not clearly observed for k_5 in the experimental uncertainty range.

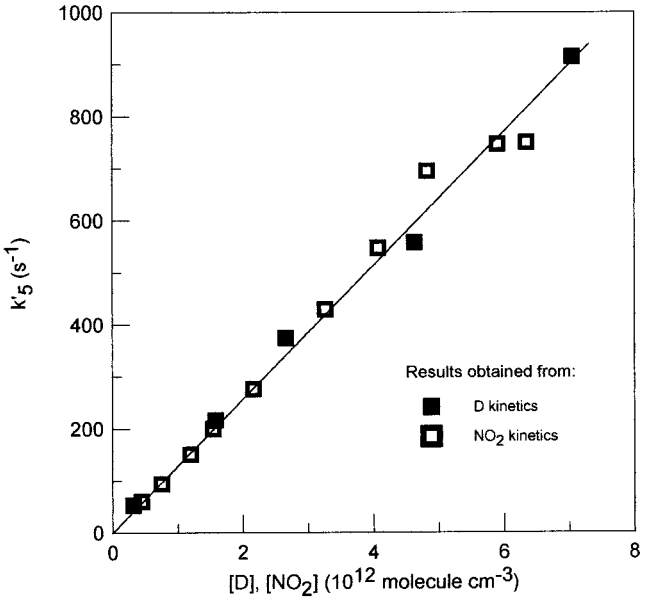

Figure 6. Reaction D + NO_2 → OD + NO (5): example of pseudo-first-order plots obtained at $T = 296$ K from D and NO_2 consumption kinetics in excess of NO_2 and D, respectively.

Discussion

In previous sections, only the bimolecular channel was considered for OH + OH and OD + OD reactions. The other

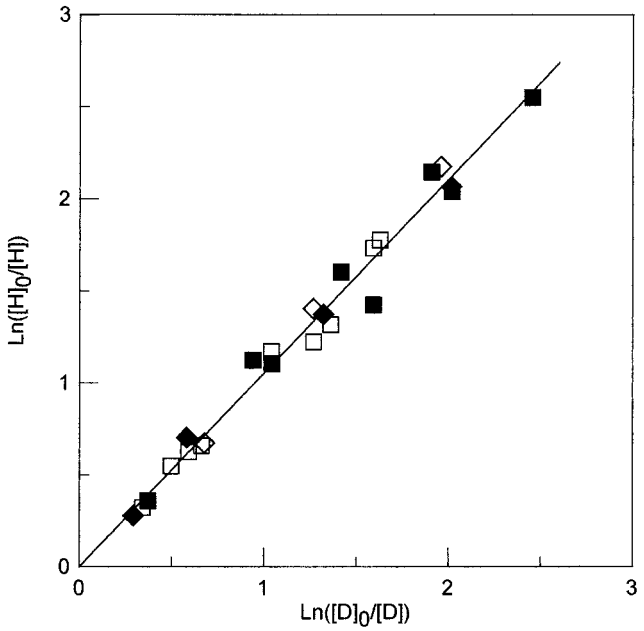

Figure 7. Reaction D + NO_2 → OD + NO (5): relative measurements of the reaction rate constant, at $T = 298$ K (open symbols) and 230 K (filled symbols) from H and D consumption kinetics (squares) and from OH and OD formation kinetics (diamonds).

channel is the association reaction:

$$OH + OH + M \rightarrow H_2O_2 + M \qquad (1')$$

$$OD + OD + M \rightarrow D_2O_2 + M \qquad (3')$$

Reaction 1′ has been studied with M = N_2,[12,15] SF_6,[16] and He.[17,18] In ref 18, the temperature dependence of the low-pressure limit for the reaction rate constant was represented by: $k_{1'} = 3.7 \times 10^{-31}[\mathrm{He}](T/300)^{-2.7}$ at $T \geq 300$ K and $k_{1'}(200\ \mathrm{K}) = 4.9 \times 10^{-31}[\mathrm{He}]$ and $k_{1'}(250\ \mathrm{K}) = 4.5 \times 10^{-31}[\mathrm{He}]$ cm^6 molecule^{-1} s^{-1}. Under the conditions of the present study (1 Torr), these data give values for $k_{1'}$ ranging from 6×10^{-15} ($T = 360$ K) to 1.9×10^{-14} cm^3 molecule^{-1} s^{-1} ($T = 233$ K). As a result, the contribution of this termolecular process (<1%) could be neglected. It is likely the case also for reaction 3′, although the contribution of the association reaction can be slightly higher.

The value of k_1 obtained in the present work can be compared with those from previous studies. Results of all the previous room-temperature data are summarized in Table 5, which is reproduced from ref 14 with addition of the results of the last three studies. As one can see, the present value of k_1 is in better agreement with the lowest values of k_1 previously measured.[5,11,13,14] The agreement with the most recent studies[13,14] appears to be very good, especially if the value $k_1 = (1.7 \pm 0.2) \times 10^{-12}$ cm^3 molecule^{-1} s^{-1} (ref 13) is likely overestimated because, as noted by the authors, the wall loss of OH was not taken into account, although the measurements were carried out in an uncoated flow tube. The main sources of error to explain the discrepancy with the other values of k_1 are the absolute determination of OH concentrations, together with the possible uncontrolled OH losses (including the heterogeneous loss).

The results of all the temperature studies of reaction 1 are shown in Figure 8. The slight negative temperature dependence of k_1 observed in the present work is in conflict with the results of Wagner and Zellner,[14] where a slight positive temperature dependence was measured at $T = 250-580$ K: $k_1 = (3.2 \pm 0.8) \times 10^{-12}\exp(-242/T)$ cm^3 molecule^{-1} s^{-1}, although the absolute values of k_1 from both studies are consistent if the stated uncertainty limits are considered. A possible explanation of the difference between the present data and those from ref 14 can be attempted. In ref 14, the value of k_1 has been measured from the flash photolysis of H_2O/N_2 mixtures and monitoring the decay of OH by UV absorption spectroscopy. The OH decay was considered to be mainly due to three reactions:

$$OH + OH \rightarrow H_2O + O \qquad (1)$$

$$OH + OH + N_2 \rightarrow H_2O_2 + N_2 \qquad (1')$$

$$O + OH \rightarrow O_2 + H \qquad (13)$$

Experiments were carried out at N_2 total pressure between 20 and 80 Torr. The values of k_1 were derived from the intercepts of the dependencies of the effective second-order rate coefficient with pressure: $k_{\mathrm{eff}} = 3k_1 + 2k_{1'}[N_2]$. Another reaction that could contribute to OH decay is:

$$OH + H\ (+N_2) \rightarrow H_2O\ (+N_2) \qquad (26)$$

The contribution of this reaction was estimated to be $0.06k_{\mathrm{eff}}$ and $0.15k_{\mathrm{eff}}$ at 20 and 60 Torr, respectively. However, this

TABLE 5: Summary of Data for Rate Constant of the Reaction OH + OH → H_2O + O at 298−300 K

k_1 (10^{-12} cm^3 molecule^{-1} s^{-1})	method[a]	reference
1.40 ± 0.30[b]	DF-UVA	5
2.57 ± 0.20	DF-ESR	6
2.08 ± 0.08	DF-ESR	7
0.84 ± 0.26	DF-ESR	7
2.3 ± 0.3	DF-ESR	9
2.1 ± 0.5	DF-ESR	10
1.4 ± 0.2	DF-RF	11
2.1 ± 0.1	FP-UVA	12
1.43 ± 0.30	FP-UVA	14
1.7 ± 0.2	DF-RF	13
1.4 ± 0.2	DF-MS	this work

[a] DF-UVA: discharge flow system−UV absorption; DF-ESR: discharge flow system−electron spin resonance; DF-RF: discharge flow system−resonance fluorescence; FP-UVA: flash photolysis−UV absorption; DF-MS: discharge flow system−mass spectrometry. [b] $T = 310$ K.

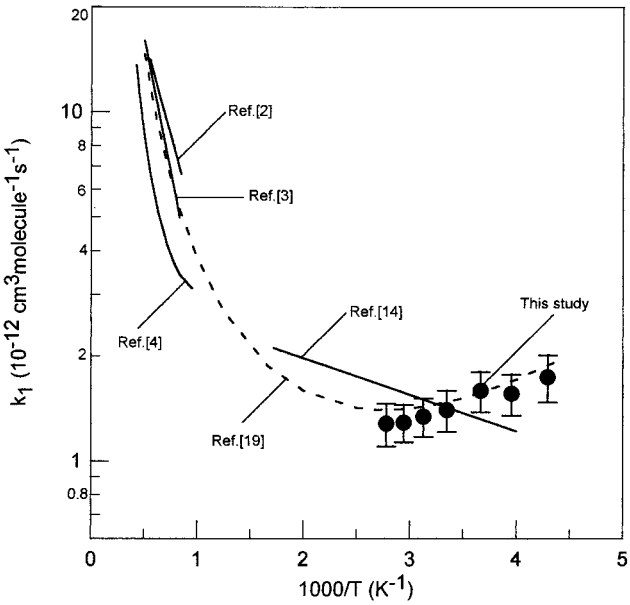

Figure 8. Reaction OH + OH → O + H_2O (1): summary of results from temperature dependence studies of the reaction rate constant.

contribution could be even higher if one considers that the value of k_{26} can be higher than that used in the calculations of ref 14: $k_{26} = 4.8 \times 10^{-31}$ cm^6 molecule^{-2} s^{-1} in ref 14, whereas the most recent evaluation[39] gives $k_{26} = 6.86 \times 10^{-31}$ $(T/298)^{-2}$ cm^6 molecule^{-2} s^{-1}. This increasing with total pressure contribution to k_{eff} could lead to underestimating the intercept of the dependence of k_{eff} on pressure, therefore resulting in an underestimation of k_1, especially at the lowest temperature of the study.[14]

In ref 19, the rate constant of reaction 1 was derived from quantum-chemical calculations. The value calculated in the temperature range 300−2000 K was: $k_1(T) = 2.04 \times 10^{-20}$ $T^{2.62}$ exp(944.9/T) cm^3 molecule^{-1} s^{-1}. The resulting data, shown in Figure 8, have been extended to the temperature range of the present work. It can be seen that these data fit well not only high- and room-temperature experimental data, but also the present data, obtained below room temperature (best fit can be obtained with a scaling factor of 0.93). In ref 19, it was argued that the rate constant calculated around room temperature "experiences the near cancellation of two conflicting influences with increasing temperature: the decrease in tunneling and the increase in surmounting the reaction barrier". The negative temperature dependence observed here for k_1 can be considered as an experimental evidence of an increase of this tunneling effect with decreasing temperature. The value of the temperature factor measured for reaction 1 in the present study: $E/R = -(210 \pm 40)$ K can be compared with those available for analogous net H-atom abstraction radical−radical reactions 27 and 28: $E/R = -(250 \pm 200)$ K and $-(600 \pm 200)$ K,[20] respectively:

$$OH + HO_2 \rightarrow H_2O + O_2 \quad (27)$$

$$HO_2 + HO_2 \rightarrow H_2O_2 + O_2 \quad (28)$$

Only one study of the OD + OD reaction has been published so far,[28] where the electron spin resonance method was used for OD absolute concentration measurements. The kinetics of OD were simulated using two variable parameters: the rate constant of reaction 3 and the heterogeneous loss rate of the radicals. The value of k_3 thus obtained at 300 K was: $k_3 = (1.49 \pm 0.16) \times 10^{-12}$ cm^3 molecule^{-1} s^{-1}. This value is higher by a factor of 3.4 than that obtained at room temperature in the present study. The possible cause for this discrepancy is likely the uncertainty in both the absolute measurements of radical concentrations and contribution of OD wall loss processes.

A significant isotopic effect is observed in the temperature range of the study for reactions 1 and 3: $k_1/k_3 = 2.9-3.7$. This seems to be in line with the reaction mechanism that has been proposed for the OH + OH reaction.[19] Both the reaction barrier and the tunneling effect do not favor the OD + OD reaction: a somewhat higher effective reaction barrier for this reaction compared with that for OH + OH can be expected because of a lower zero-point energy of the reactants and, second, the tunneling contribution to the rate constant is lower for the heavier isotope. From another side, this lower tunneling contribution implies that the temperature dependence of the rate constant for OD + OD reaction is determined mainly by the reaction barrier, and a positive temperature dependence of k_3 should be expected. As shown above, a slight negative temperature effect ($E/R = 170 \pm 60$ K) is observed for k_3 in the present experiments (although k_3 can be presented as a temperature-independent value with $k_3 = (4.5 \pm 0.5) \times 10^{-13}$ cm^3 molecule^{-1} s^{-1} within the uncertainty limits of the study). Finally, theoretical calculations (similar to those for the OH + OH reaction) would be very useful to understand the reaction mechanism and the relative role of the different factors determining the temperature behavior of the rate constant.

It is interesting to compare the observed kinetic isotope effect with that known for reactions $HO_2 + HO_2$ (28)[40,41] and $OH + H_2O_2$ (29):[42]

$$HO_2 + HO_2 \rightarrow H_2O_2 + O_2 \quad (28)$$

$$DO_2 + DO_2 \rightarrow D_2O_2 + O_2 \quad (28a)$$

$$OH + H_2O_2 \rightarrow HO_2 + H_2O \quad (29a)$$

$$OH + D_2O_2 \rightarrow \text{products} \quad (29b)$$

$$OD + D_2O_2 \rightarrow \text{products} \quad (29c)$$

$$OD + H_2O_2 \rightarrow \text{products} \quad (29d)$$

The reaction of OH with H_2O_2 and their isotopic analogues has been studied by Vaghjiani et al.,[42] leading to $k_{29a} = k_{29d}$ and $k_{29b} = k_{29c}$. Besides, the kinetic isotopic effects, $k_{29a}/k_{29c} = 2.7-3.5$ (ref 42) and that measured for reactions 28 and 28a, $k_{28}/k_{28a} = 2.8$ (ref 40) and 3.3 (ref 41), are the same as that observed in the present study: $k_1/k_3 = 2.9-3.7$.

The rate coefficients for the reactions OH + OH and OH + OD have been found to be the same within the experimental uncertainty limits. It can be noted that, usually, OH and OD have the same rate coefficients for exothermic hydrogen-abstraction reactions, as it was observed, for example, for the reactions of OH with H_2O_2,[42] CH_3OOH,[43] H_2,[44] n-C_4H_{10},[45] and HI.[46] However, the case of the OH + OD reaction seems to be different because there are two different pathways for this reaction, both leading to the formation of the same products (O and HOD): H atom transfer (transition state [DOHO]¶) and D atom transfer (transition state [HODO]¶). Considering the significant kinetic isotope effect measured in the present study for reactions 1 and 3, one can expect the lower probability for the D atom abstraction compared with the H atom abstraction and, consequently, a lower rate constant for the OH + OD reaction compared with that for reaction 1. Considering a purely statistical H-atom and D-atom transfer mechanism for reaction 4, the value of k_4 should have been $k_4 = 0.5 \times (k_1 + k_3) = (0.9 \pm 0.1) \times 10^{-12}$ cm^3 molecule^{-1} s^{-1} at $T = 298$ K compared with the experimental value $k_4 = (1.5 \pm 0.3) \times 10^{-12}$ cm^3 molecule^{-1} s^{-1}. Although the difference between these two values is low, considering the uncertainty ranges, it seems to be significant and this would be checked by theoretical calculations.

In conclusion, the kinetic information provided by the present work for the OH + OH and OD + OD reactions extends the existing kinetic database and can be used for further theoretical development.

Acknowledgment. This study has been carried out within a project funded by the European Commission within the Environment and Climate Program (contract ENV−CT97−0576).

References and Notes

(1) Mallard, W. G.; Westley, F.; Herron, J. T.; Hampson, R. F. *NIST Chemical Kinetics Data Base, ver. 6.0*; NIST Standard Reference Data, Gaithersburg, MD, 1994.

(2) Rawlins, W. T.; Gardiner, W. C. *J. Chem. Phys.* **1974**, *60*, 4676.

(3) Ernst, J.; Wagner, H. Gg.; Zellner, R. *Ber. Bunsen-Ges. Phys. Chem.* **1977**, *81*, 1270.

(4) Wooldridge, M. S.; Hanson, R. K.; Bowman, C. T. *Int. J. Chem. Kinet.* **1994**, *26*, 389.
(5) Del Greco, F. P.; Kaufman, F. *Discuss. Faraday Soc.* **1962**, *33*, 128.
(6) Dixon-Lewis, G.; Wilson, W. E.; Westenberg, A. A. *J. Chem. Phys.* **1966**, *44*, 2877.
(7) Wilson, W. E.; O'Donovan, J. T. *J. Chem. Phys.* **1967**, *47*, 5455.
(8) Breen, J. E.; Glass, G. P. *J. Chem. Phys.* **1970**, *52*, 1082.
(9) Westenberg, A. A.; De Haas, N. *J. Chem. Phys.* **1973**, *58*, 4006.
(10) McKenzie, A.; Mulkahy, M. F. R.; Steven, J. R. *J. Chem. Phys.* **1973**, *59*, 3244.
(11) Clyne, M. A. A.; Down, S. *J. Chem. Soc., Faraday Trans. 2* **1974**, *70*, 253.
(12) Trainor, D. W.; von Rosenberg, C. W. *J. Chem. Phys.* **1974**, *61*, 1010.
(13) Farquharson, G. K.; Smith, R. H. *Aust. J. Chem.* **1980**, *33*, 1425.
(14) Wagner, G.; Zellner, R. *Ber. Bunsen-Ges. Phys. Chem.* **1981**, *85*, 1122.
(15) Zellner, R.; Ewig, F.; Paschke, R.; Wagner, G. *J. Phys. Chem.* **1988**, *92*, 4184.
(16) Fagerstrom, K.; Lund, A.; Mahmound, G.; Jodkowski, J. T.; Ratajczac, E. *Chem. Phys. Lett.* **1994**, *224*, 43.
(17) Forster, R.; Frost, M.; Fulle, D.; Hamann, H. F.; Hippler, H.; Schlepegrell, A.; Troe, J. *J. Chem. Phys.* **1995**, *103*, 2949.
(18) Fulle, D.; Hamann, H. F.; Hippler, H.; Troe, J. *J. Chem. Phys.* **1996**, *105*, 1001.
(19) Harding, L. B.; Wagner, A. F. *22nd International Symposium on Combustion*; The Combustion Institute, Pittsburgh, 1988; p 983.
(20) De More, W. B.; Sander, S. P.; Golden, D. M.; Hampson, R. F.; Kurylo, M. J.; Howard, C. J.; Ravishankara, A. R.; Kolb, C. E.; Molina, M. J. *Chemical Kinetics and Photochemical Data for Use in Stratospheric Modeling*; NASA, JPL, California Institute of Technology: Pasadena, CA, 1997.
(21) Atkinson, R.; Baulch, D. L.; Cox, R. A.; Hampson, R. F.; Kerr, J. A.; Rossy, M. J.; Troe, J. *J. Phys. Chem. Ref. Data* **1997**, *26*, 521.
(22) Chipperfield, M. P.; Shallcross, D. E.; Lary, D. J. *Geophys. Res. Lett.* **1997**, *24*, 3025.
(23) Chartland, D. J.; McConnell, J. C. *Geophys. Res. Lett.* **1998**, *25*, 55.
(24) Bogan, D. J.; Thorn, R. P.; Nesbitt, F. L.; Stief, L. J. *J. Phys. Chem.* **1996**, *100*, 14838.
(25) Bedjanian, Y.; Le Bras, G.; Poulet, G. *Int. J. Chem. Kinet.*, in press.
(26) Lipson, J. B.; Elrod, M. J.; Beiderhase, T. W.; Molina, L. T.; Molina, M. J. *J. Chem. Soc., Faraday Trans.* **1997**, *93*, 2665.
(27) Chase, M. W. *J. Phys. Chem. Ref. Data Monogr.* **1998**, *1*.
(28) Westenberg, A. A.; Wilson, W. E.. *J. Chem. Phys.* **1966**, *45*, 338.
(29) Gilles, M. K.; Kegly-Owen, C.; McCabe, D.; Burkholder, J. B.; Ravishankara, A. R. *Book of Abstracts*, 15th International Symposium on Gas Kinetics, Bilbao, September, 1998; The University of the Basque Country: Bilbao, Spain, 1998; B2, p 22.
(30) Bedjanian, Y.; Le Bras, G.; Poulet, G. *Chem. Phys. Lett.* **1997**, *266*, 233.
(31) Kukui, A.; Kirchner, U.; Benter, T.; Schindler, R. N. *Ber. Bunsen-Ges. Phys. Chem.* **1996**, *100*, 455.
(32) Nicovich, J. M.; Wine, P. H. *Int. J. Chem. Kinet.* **1990**, *22*, 379.
(33) Wada, Y.; Takayanagi, T.; Umemoto, H.; Tsunashima, S.; Sato, S. *J. Chem. Phys*. **1991**, *94*, 4896.
(34) Bossard, A. R.; Singleton, D. L.; Paraskevopoulos, G. *Int. J. Chem. Kinet.* **1988**, *20*, 609.
(35) Singleton, D. L.; Paraskevopoulos, G.; Irwin, R. S.. *J. Phys. Chem.* **1991**, *95*, 694.
(36) Kaufman, F. *J. Phys. Chem.* **1984**, *88*, 4909.
(37) Morrero, T. R.; Mason, E. A. *J. Phys. Chem. Ref. Data* **1972**, *1*, 3.
(38) Howard, M. J.; Smith, I. W. M. *J. Chem. Soc., Faraday Trans. 2* **1982**, *78*, 1403.
(39) Baulch, D. L.; Cobos, C. J.; Cox, R. A.; Esser, C.; Frank, P.; Just, Th.; Kerr, J. A.; Pilling, M. J.; Troe, J.; Walker, R. W.; Warnatz, J. *J. Phys. Chem. Ref. Data* **1992**, *21*, 411.
(40) Hamilton, E. J.; Lii, R.-R. *Int. J. Chem. Kinet.* **1977**, *9*, 875.
(41) Sander, S. P.; Peterson, M.; Watson, R. T. *J. Phys. Chem.*, **1982**, *86*, 1236.
(42) Vaghjiani, G. L.; Ravishankara, A. R.; Cohen, N. *J. Phys. Chem.* **1989**, *93*, 7833.
(43) Vaghjiani, G. L.; Ravishankara, A. *J. Phys. Chem.* **1989**, *93*, 1948.
(44) Talukdar, R. K.; Gierczak, T.; Goldfarb, L.; Rudich, Y.; Madhara Rao, B. S.; Ravishankara, A. R. *J. Phys. Chem.* **1996**, *100*, 3037.
(45) Paraskevopoulos, G.; Nip, W. S. *Can. J. Chem.* **1980**, *58*, 2146.
(46) Butkovskaya, N. I.; Setser, D. W. *J. Chem. Phys.* **1997**, *106*, 5028.